

Indirect Electrochemical Cr(III) Oxidation in KOH Solutions at an Au Electrode: The Role of Oxygen Reduction Reaction

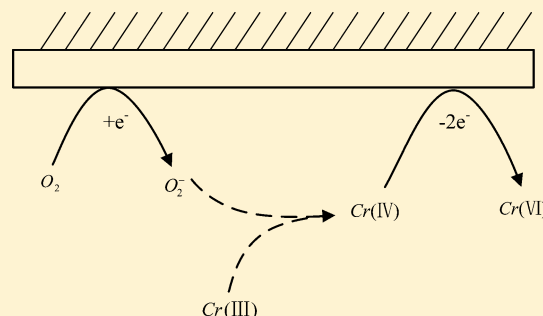
Wei Jin,^{†,§} Michael S. Moats,[‡] Shili Zheng,[†] Hao Du,^{*,†} Yi Zhang,[†] and Jan D. Miller[‡]

[†]National Engineering Laboratory for Hydrometallurgical Cleaner Production Technology, Institute of Process Engineering, Chinese Academy of Sciences, Beijing, 100190, People's Republic of China

[‡]Department of Metallurgical Engineering, University of Utah, Salt Lake City, Utah 84112, United States

[§]Graduate School, Chinese Academy of Sciences, Beijing, 100049, People's Republic of China

ABSTRACT: The indirect electro-oxidation of Cr(III) by in situ generated superoxide at a gold electrode has been investigated in KOH solutions using cyclic voltammetry and UV–vis spectroscopy. It is observed that the indirect Cr(III) oxidation behavior is substantially affected by the media pH and there is a pH-modulated oxygen reduction reaction (ORR) process to generate reactive oxygen species which promotes Cr(III) oxidation. The ORR in KOH solutions is attributed to a quasi-reversible diffusion-controlled reaction. In dilute KOH solution (0.2 M), 4e[−] reduction occurs and no reactive oxygen species are generated for the indirect Cr(III) oxidation. Moreover, Cr(III) oxidation is inhibited due to competition for the electrode active sites. As the alkaline concentration increases (3.0 M), the protonation of superoxide is greatly suppressed, and thus, 1e[−] ORR to generate superoxide is observed. This change in mechanism facilitates the indirect Cr(III) oxidation through the superoxide as a mediator to oxidize Cr(III) to Cr(IV), which is the rate-determining step of Cr(III) oxidation to Cr(VI).



1. INTRODUCTION

The redox cycle of chromium compounds in solid and aquatic environment has attracted considerable interest over recent years due to its great importance in natural phenomena^{1,2} and industrial processes.^{3,4} Cr exhibits two stable oxidation states, Cr(III) and Cr(VI). Each state has significantly different physicochemical properties³ and biochemical reactivity.⁵ Cr(III) compounds are relatively harmless, but their mobility is limited by their low solubility in the aqueous system.⁶ In contrast, Cr(VI) compounds are very soluble and mobile with extreme toxicity and carcinogenicity.⁷ Recently, owing to the widespread application in mineral processing, solid waste remediation, and biologic science, the oxidation behavior of Cr(III) to Cr(VI) has garnished scientific interest.^{8–11}

Due to the high redox potential of the Cr(VI)/Cr(III) couple, only a few oxidants are capable of oxidizing Cr(III) to Cr(VI), such as cerium(IV)¹² and Mn-bearing compounds,^{13,14} while dissolved oxygen is confirmed to be ineffective.³ Recently, efforts have been made for mineral processing purposes to evaluate other potential oxidants, which can effectively oxidize Cr(III) without inputting additional elements to the aqueous system. Rao¹⁵ and Pettine¹⁶ studied the oxidation of Cr(III) by hydrogen peroxide (H₂O₂) and found that its kinetics are strongly influenced by the media pH. Zhao¹⁷ observed that the OH/O[−] radical also can act as a Cr(III) oxidation agent in alkaline solution. Zhang¹⁸ discovered that Cr(III) oxidation by OH• radical was significantly limited at pH below 2.5 or above 5.0, while the OH• radical was generated by light-induced

photolysis of Fe(OH)²⁺ complexes, resulting in the accumulation of Fe compounds in the system. Moreover, it has been suggested that Cr(III) could rapidly react with other free radicals such as HO₂ and O₂^{•−}.¹⁹ However, these advanced oxidation processes (AOP) have several drawbacks such as low capacity chemical destruction level, storage and/or transportation of dangerous reactants, and high investment cost.²⁰

Electrochemical oxidation could be an attractive alternative method for Cr(III) oxidation, benefiting from its efficiency, versatility, easy manipulation, environmental compatibility, and cost-effectiveness.²¹ There are two electrochemical techniques commonly used for electro-oxidation processes: direct oxidation and indirect oxidation.^{20,22} Direct electrochemical oxidation involves exchange of electrons directly with the electrode surface. Indirect oxidation proceeds through the generation and consumption of some strong oxidants. While similar to the chemical destruction mentioned previously, the oxidants are electro-generated in situ in the system and act as intermediary agents for electron exchange between the electrode and the ions to be oxidized.

The oxidation mediators can be metallic redox couples or powerful oxidized agents,²³ such as active chlorine, ozone, H₂O₂, persulfate (S₂O₈^{2−}), and percarbonate (C₂O₆^{2−}). Among these mediators, the reactive oxygen species (ROS) in situ

Received: April 6, 2012

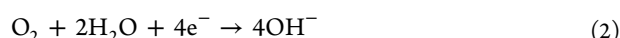
Revised: June 4, 2012

Published: June 5, 2012

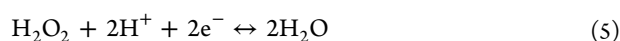


electro-generated via reduction of molecular oxygen,^{24,25} such as H_2O_2 , is widely used because it is a strong oxidant and leaves no residual after indirect oxidation occurs. However, the reactive species production from oxygen reduction reaction (ORR) is significantly determined by the electrode material and electrolyte condition, especially the media pH.²⁶

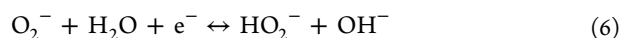
It has been demonstrated that the ORR could happen via two pathways, which are “direct” 4e reduction and “series” reduction.^{27,28} The “direct” pathway is one-step 4e reduction of oxygen to H_2O in acidic solution or OH^- in basic solution, as illustrated in eqs 1 and 2, respectively, where no reactive intermediate or product could be generated.



In contrast, during the “series” reduction process, oxygen is first reduced to superoxide anion, as shown in eq 3, followed by further reduction steps to hydrogen peroxide molecule (H_2O_2) and H_2O (eqs 4 and 5, respectively) in acidic media



or to hydrogen peroxide anion (HO_2^-) and OH^- (eqs 6 and 7, respectively) in basic media.



In this scheme, the reactive oxygen species, such as HO_2^- and O_2^- in alkaline solution, could exist as intermediates or products depending on the electrode material and reaction media, and thus may be employed as an oxidation mediator in the indirect electro-oxidation of Cr(III). Besides, it should be noted that few investigations have been reported on the effective oxidation activity of in situ electro-generated O_2^- via ORR. Fei²⁹ found the arsenite oxidation by superoxide at a TiO_2 electrode in acidic media is ineffective and needs additional UV illumination to transfer O_2^- into other derivatives. This is possibly because superoxide is only stable in concentrated alkaline solutions or aprotic media.^{30,31}

Direct Cr(III) electrochemical oxidation has been studied at Pt,³² Au,³³ and MnO_2 ³⁴ electrodes, and most of these investigations were carried out under alkaline conditions. Jin¹¹ identified the pH-dependent mechanism transition for the electro-oxidation of Cr(III) and found that increasing the pH facilitates oxidation in the KOH solution in concentrations ranging from 0.1 to 3.0 M.

Limited information on the indirect electro-oxidation of Cr(III) is available. In this regard, the aim of this study is to elucidate the mechanism regarding the electrolyte-dependent effect on ORR and investigate the indirect electrochemical oxidation behavior of Cr(III) by ROS, especially superoxide (O_2^-) generated in situ via ORR in KOH solutions.

2. EXPERIMENTAL PROCEDURES

$\text{Cr}(\text{NO}_3)_3$ (99.99% mass fraction, Sigma-Aldrich) and KOH stock solution (45% mass fraction, HPLC grade, Sigma-Aldrich, total impurities $\text{K}_2\text{CO}_3 \leq 0.3\%$ mass fraction) were used without further purification. All solutions were prepared with

purified Milli-Q water ($18 \text{ M}\Omega \text{ cm}$) at $25 \pm 0.2^\circ \text{C}$ in a nitrogen-filled glovebox to minimize contamination by CO_2 .³⁵ Besides, the Cr(III)-bearing KOH solutions were prepared immediately before reaction to avoid polymerization, a complex process which occurs over time scales from hours to days.³⁶

Cyclic voltammetry (CV) experiments were conducted in a 150 mL three-electrode electrochemical cell at $25 \pm 0.2^\circ \text{C}$ using a Modulab (Solartron Analytical) electrochemical workstation. A gold (99.99% purity, polycrystalline, 0.23 cm^2 effective area) cylinder electrode was employed as the working electrode, while a large-area Pt foil was used as the counter electrode. All potentials were measured and presented versus a saturated calomel electrode (SCE). Prior to each measurement, the gold electrode was polished with decreasing sizes of alumina powder ($1.0\text{--}0.3 \mu\text{m}$) to obtain a mirror-like surface. Following polishing, the electrode was sonicated in water to remove the trace alumina. The gold electrode was then electrochemically activated by cycling between the onset potential of H_2 and O_2 evolution reactions in the corresponding N_2 -saturated KOH solution until reproducible and well-defined CV curves were observed. The electrochemical measurements were then performed in either N_2 -purged or O_2 -saturated alkaline solutions by potential cycling from -0.95 to 0.65 V for 0.2 M KOH and from -0.95 to 0.49 V for 3.0 M KOH solutions, respectively. The upper limit of potential cycling was chosen from below the O_2 evolution potential region. When the number of potential cycles employed was very high, the gold electrode was washed, polished, and electrochemically pretreated after every 300 cycles to decrease the poisoning effect²⁰ due to the formation of an oxide layer on the electrode surface. Besides, owing to the relatively small difference between Cr(III) oxidation peak current in N_2 -purged and O_2 -saturated KOH solutions, the scan rate in most figures was set at 200 mV/s to obtain a large peak current.

The concentration of Cr(VI) obtained after corresponding cycles was determined using a Labtech model 9100B double beam UV-vis spectrophotometer at a 1 nm/s scanning rate from 190 to 600 nm . It was quantified by measuring the characteristic absorbance of Cr(VI) at 372 nm ,³⁷ while the molar extinction coefficients of Cr(VI) are 5216 and $5994 \text{ M}^{-1}\cdot\text{cm}^{-1}$ in 0.2 and 3 M KOH , respectively (the solution path length is 1.0 cm).

3. RESULTS AND DISCUSSION

3.1. Direct Electro-Oxidation of Cr(III) in KOH Solutions. At the gold electrode, Cr(III) oxidation has been shown to be electrochemically active only in very alkaline solution ($\text{pH} > 12$),³³ where the Cr(III) is present as CrO_2^- . Figure 1a shows the cyclic voltammetry (CV) curve of 1.0 mM Cr(III) and its corresponding blank curve in N_2 -purged 0.2 M KOH solution at 200 mV/s . As shown in the CV curve in 0.2 M KOH solution (blank), the broad wave commencing at -0.48 V is attributed to the OH^- adsorption.^{35,38} The oxide formation peak occurs at 0.33 V , and the oxide reduction peak emerges at 0.05 V in the negative-going sweep, which is followed by the desorption of chemisorbed OH^- at more negative potentials.^{35,38} In the presence of Cr(III), the oxidation peak at 0.06 V is attributed to the Cr(III) oxidation, while its corresponding Cr(VI) reduction peak is observed at -0.57 V . Clearly, the large peak potential separation ΔE_p ($\Delta E_p = E_{pa} - E_{pc}$, in which E_{pa} and E_{pc} are the anodic peak potential and the cathodic peak potential, respectively) and low peak current ratio i_{pc}/i_{pa} (i_{pc} and i_{pa} are the anodic peak current and

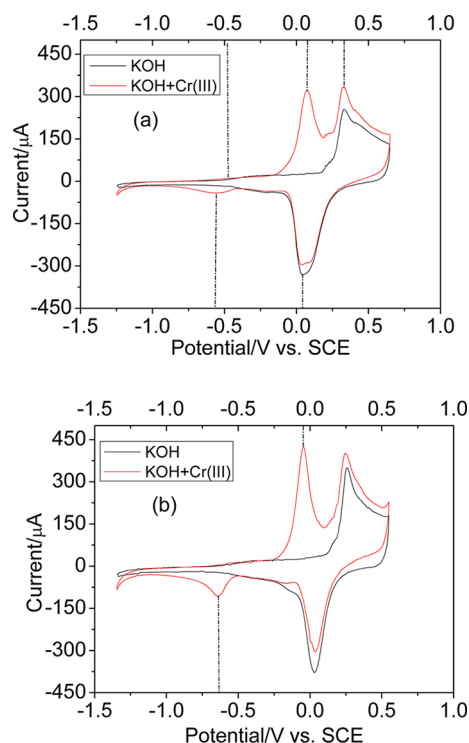
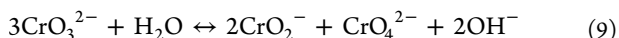
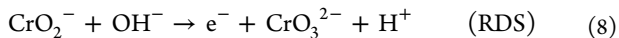


Figure 1. Cyclic voltammograms of the first cycle in the presence (red) and absence (black) of 1.0 mM Cr(III) in (a) 0.2 M and (b) 3.0 M KOH deaerated solutions at a gold electrode, respectively; scan rate = 200 mV/s.

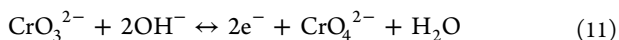
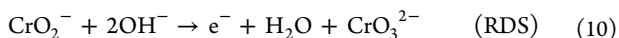
the cathodic peak current, respectively) of these couple peaks indicate a pseudoirreversible reaction. It should be noted that the increase in the oxidation current at 0.33 V originates from the “tail” of the Cr(III) oxidation wave and is not attributed to increased gold oxide formation. Additionally, the peak current for the reduction of gold oxide at 0.05 V decreases owing to the passivating effect of chromium.³⁹

According to our previous study,¹¹ the Cr(III) oxidation mechanism in deaerated 0.2 M KOH solution is as follows:



The electro-oxidation is initiated by a 1e electron transfer which is the rate-determining step (RDS), followed by the relatively fast disproportionation reaction to produce Cr(VI).

The Cr(III) oxidation behavior is substantially influenced by the media pH, and the disproportionation step is replaced by further fast 2e electron transfer in deaerated 3.0 M KOH solution, which leads to a stepwise three-electron-transfer process as follows:¹¹



The first electron transfer is the RDS, and this pH-dependent mechanism transition favors the Cr(III) oxidation thermodynamics and kinetics. As shown in Figure 1b, with the increasing KOH concentration, the Cr(III) oxidation peak potential negatively shifts to −0.05 V due to the involvement of OH[−] in the RDS, and the anodic peak current increases from 300 to 405 μA owing to the further fast 2e electron transfer.

Furthermore, the peak potential separation ΔE_p for the Cr(III)/Cr(VI) couple decreases from 0.63 V in 0.2 M KOH solution to 0.58 V in 3.0 M KOH solution and the peak current ratio i_{pc}/i_{pa} increases from 0.06 to 0.19, indicating an increase in reversibility and the existence of a mechanism transition.

3.2. Oxygen Reduction Reaction in KOH Solution. The oxygen reduction reaction carried out in oxygen-saturated 0.2 and 3.0 M KOH solutions with their corresponding blank curves under N₂ atmosphere are illustrated in Figure 2a and b,

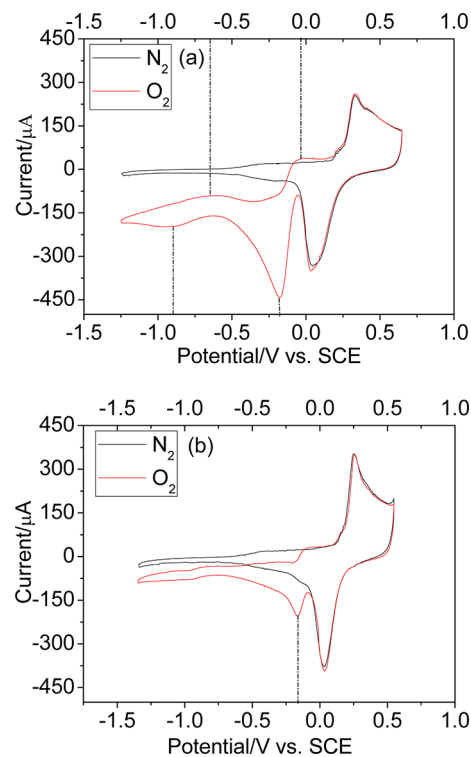


Figure 2. The CV curves (first cycle) of ORR at a gold electrode in (a) 0.2 M and (b) 3.0 M KOH solution, respectively; scan rate = 200 mV/s.

respectively. In Figure 2a, the peak at −0.18 V is assigned to the reduction of O₂ to HO₂[−] via the overall reaction of (3) and (6) mentioned above, while the peak at −0.89 V to the reduction of HO₂[−] to OH[−], their corresponding counter reactions emerge at −0.06 and −0.63 V, respectively,⁴⁰ exhibiting quasi-reversible reaction characteristics. The ORR in 0.2 M KOH solution is attributed to a series 4e reduction with HO₂[−] as an intermediate. Besides, the HO₂[−] can further disproportionate to OH[−] (as shown in eq 12) and produce an apparent 4e reduction.⁴¹ Consequently, the HO₂[−] is immediately removed and cannot be detected, suggesting possibly no contribution to the indirect oxidation of Cr(III) in the following section.



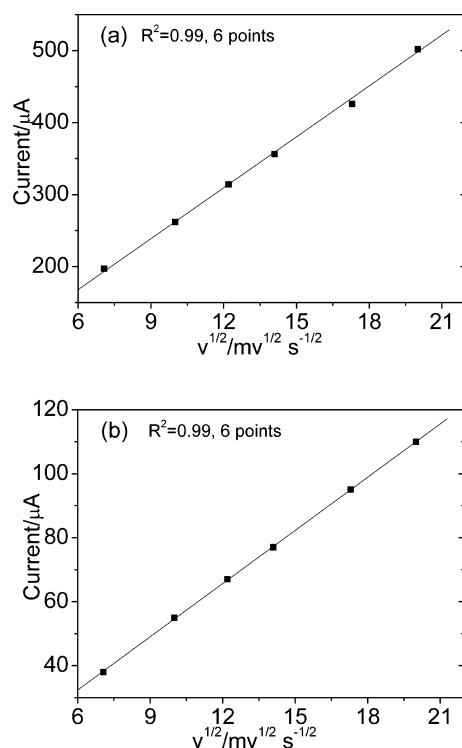
The ORR behavior is greatly determined by media condition both in kinetics and mechanism considerations. As compared to the ORR peak at −0.18 V in 0.2 M KOH, the peak potential in 3.0 M KOH slightly positively shifts to −0.17 V, while the peak current significantly decreases from 356 to 77 μA, as illustrated in Table 1, indicating the inhibition of the ORR kinetics due to the increase in alkaline concentration. Moreover, the further reduction peak becomes too broad and weak to distinguish, suggesting the mechanism has possibly changed.

Table 1. Comparison of ORR Behavior in 0.2 and 3.0 M KOH Solutions

KOH (M)	E_p (V)	i_p (μ A)	n	E_{pf}^a (V)	i_{pf}^b (μ A)
0.2	−0.18	356	1.90	−0.88	40
3.0	−0.17	77	1.12		

^aThe peak potential of further reduction. ^bThe peak current of further reduction.

Due to the lack of published ORR data in concentrated alkaline solution at a gold electrode, CV curves with different scan rates (from 50 to 400 mV/s) in 0.2 and 3.0 M KOH solutions were recorded to gather kinetic and mechanism information. As illustrated in Figure 3, there is a linear

**Figure 3.** The variation of ORR peak current as a function of the square root of scan rates (50–400 mV/s) in (a) 0.2 M KOH solution at −0.18 V and (b) 3.0 M KOH solution at −0.17 V, respectively.

relationship between the peak current and $v^{1/2}$ for ORR in both 0.2 M KOH solution at −0.18 V and 3.0 M KOH solution at −0.17 V, indicating a diffusion-controlled reaction characteristic. It is known that O_2 is the main reaction species in the ORR regardless of the reaction mechanism; therefore, the ORR kinetics is mainly determined by the mass transport of O_2 , which is closely related to the solubility and diffusion properties. As the alkaline concentration increases, the oxygen solubility and diffusion coefficient decrease,^{11,26} leading to the decrease in ORR current observed.

The peak current of a diffusion controlled quasi-reversible reaction at 298 K can be calculated using the Randles–Sevcik equation:

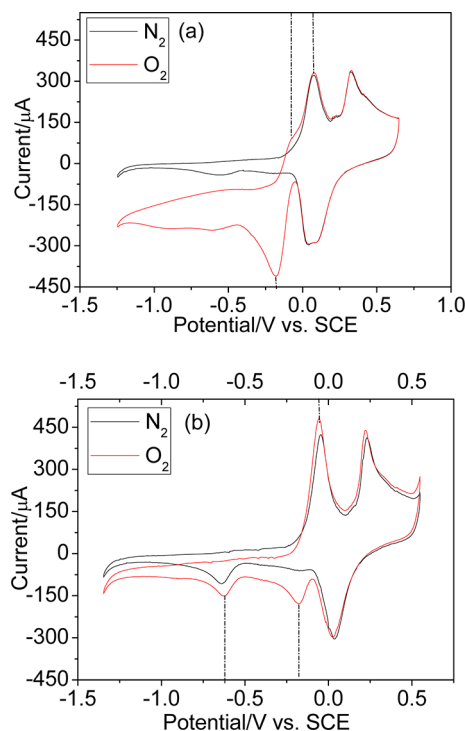
$$i_p = (2.69 \times 10^5) n^{3/2} A D_{O_2}^{1/2} C_{O_2} v^{1/2} \quad (13)$$

where i_p is the ORR peak current, n is the number of electrons, A is the surface area of the working electrode, D_{O_2} is the diffusion coefficient of the oxygen, C_{O_2} is the solubility of

oxygen, and v is the scan rate. Consequently, the electron transfer numbers (n) for the first ORR peak were obtained and presented in Table 1 using previously reported D_{O_2} and C_{O_2} data.⁴² Obviously, there is a transition of n from ~ 2 in 0.2 M to ~ 1 in 3.0 M KOH solutions, indicating the first step of the ORR reaction pathway shifts from 2e reduction to 1e reduction (as shown in eq 3). As previously discussed, in dilute KOH, the 2e reduction leads to oxygen intermediates that further reduced or quickly disproportionate, resulting in the 4e transfer mechanism.

This electrolyte-dependent effect on reaction pathway likely stems from the protonation of O_2^- , as illustrated in eq 6. In alkaline solutions, H_2O is the proton source that reacts with O_2^- to generate HO_2^- , and with the increasing alkaline concentration, the protonation of superoxide is greatly suppressed owing to the increase of OH^- concentration and decrease in H_2O , and thus 1e ORR to produce superoxide is dominating, as illustrated in eq 3. This conclusion is consistent with the previous investigations at Pt electrode in alkaline solutions.²⁶ Consequently, the superoxide is generated and stably exists and thus possibly acts as a mediator for the indirect oxidation of Cr(III) in the following section.

3.3. Indirect Electro-Oxidation of Cr(III). To examine the influence of ORR on the electro-oxidation behavior of Cr(III), cyclic voltammetry curves were generated for 1.0 mM Cr(III), N_2 -purged and O_2 -saturated KOH solutions. These curves are presented in Figure 4. In 0.2 M KOH solution, as shown in Figure 4a, the ORR-related peaks are nearly the same with or without Cr(III) present (see Figure 3a), indicating no reaction occurs between the ORR species and Cr(III). Moreover, the Cr(III) oxidation peak current decreases from 300 μ A in N_2 -purged solution to 243 μ A in O_2 -saturated solution due to the

**Figure 4.** Cyclic voltammograms (first cycle) of 1.0 mM Cr(III) in the N_2 (black) and O_2 (red) saturated (a) 0.2 M and (b) 3.0 M KOH solution at a gold electrode, respectively; scan rate = 200 mV/s.

competitive effect between Cr(III) oxidation and the corresponding oxidation of ORR.

In contrast, the corresponding oxidation peak of ORR disappears in 3.0 M KOH solution, as shown in Figure 4b, suggesting the superoxide reacts with Cr-bearing species. Meanwhile, the peak current for Cr(III) oxidation increases from 405 μA in N_2 -purged solution to 491 μA in O_2 -saturated solution, while its corresponding Cr(VI) reduction peak current remains constant at 70 μA , resulting in a decrease in the peak current ratio $i_{\text{pc}}/i_{\text{pa}}$. This indicates the indirect oxidation effect of ORR toward Cr(III) oxidation.

To further investigate the indirect oxidation effect, the chemical reaction coupled to charge transfers can be determined from the dependence of the function $i_{\text{p}}/(v^{1/2})$ on scan rate,⁴³ as illustrated in Figure 5. Obviously, over the entire

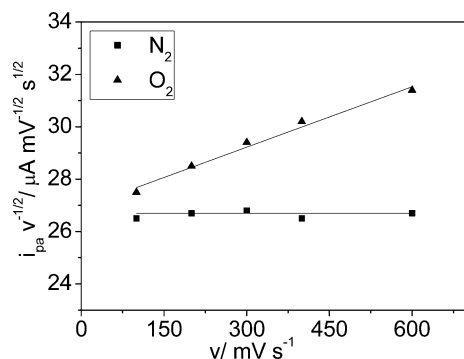


Figure 5. The dependence of anodic peak current function on the scan rate (100–600 mV/s) of 1.0 mM Cr(III) electro-oxidation in 3.0 M KOH solutions at a gold electrode.

range of scan rates, the quantity of $i_{\text{p}}/(v^{1/2})$ is constant in N_2 -purged 3.0 M KOH solution, indicating the system involves only multistep charge transfers. The monotonical increase of $i_{\text{p}}/(v^{1/2})$ with scan rate in corresponding O_2 -saturated solution indicates the involvement of a chemical step. This chemical step is believed to be the indirect oxidation of Cr(III) by a reactive oxygen species, i.e., superoxide, that is generated via the ORR in O_2 -saturated 3.0 M KOH solution.

The oxidation products generated under different conditions are determined by UV–vis absorption spectra as a function of voltammetry cycle. The spectra data are presented in Figure 6. In O_2 saturated 0.2 M KOH solution, the Cr(VI) characteristic absorbance at 372 nm, as shown in Figure 6a, clearly provides spectroscopic evidence for Cr(VI) as the Cr(III) electro-oxidation product. In Figure 6b and c, there is a good linear relationship between the Cr(VI) concentration produced and the number of potential cycles.

Obviously, the Cr(III) oxidation is greatly influenced by this electrolyte-dependent ORR. In 0.2 M KOH solution, the ORR proceeds as 4e reduction and no reactive oxygen species was stably generated; thus, no indirect oxidation effect on Cr(III) occurs. Moreover, due to the competitive effect of the corresponding oxidation of ORR on electrode active sites, the Cr(III) oxidation was inhibited, resulting in less Cr(VI) formation as compared to that in the corresponding N_2 atmosphere, as shown in Figure 6b. In contrast, there is a significant indirect oxidation effect on Cr(III) by ORR in 3.0 M KOH solution and more Cr(VI) was produced in O_2 -saturated solution, as shown in Figure 6c. Again, it is believed that the production of superoxide acts as an oxidation mediator in the

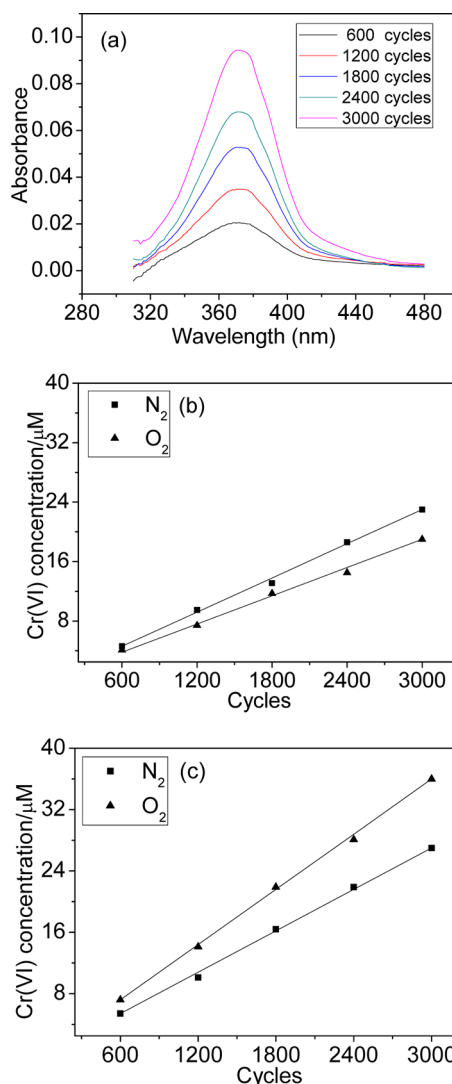


Figure 6. The Cr(VI) generated in 1.0 mM Cr(III) alkaline solutions at a gold electrode: (a) the UV–vis spectra after different potential cycles in O_2 -saturated 0.2 M KOH solution; (b) the comparison of Cr(VI) generated in N_2 and O_2 saturated 0.2 M KOH solution; (c) the comparison of Cr(VI) generated in N_2 and O_2 3.0 M KOH solution; scan rate = 200 mV/s.

more alkaline solution. Consequently, the indirect Cr(III) oxidation behavior is dependent on whether the reactive oxygen species can be in situ generated by ORR.

3.4. Proposed Mechanism of Superoxide-Driven Indirect Oxidation. As mentioned above, the electro-oxidation mechanism of Cr(III) in N_2 -purged 3.0 M KOH solution is the rate-determining first electron transfer followed by further 2e fast electron transfer. In corresponding O_2 -saturated solution, superoxide is in situ generated via 1e oxygen reduction reaction and acts as an oxidation mediator to enhance the Cr(III) oxidation.

According to previous studies, the superoxide-mediated oxidation generally occurs through a 1e pathway, such as As(III) to As(IV),²⁹ Mn(II) to Mn(III),⁴⁴ etc. Consequently, the mechanism of superoxide-driven indirect Cr(III) oxidation is possibly 1e chemical oxidation to yield Cr(IV), as shown in eq 14, and thus accelerates the RDS reaction, followed by fast 2e electron transfer to produce Cr(VI). Figure 7 presents the

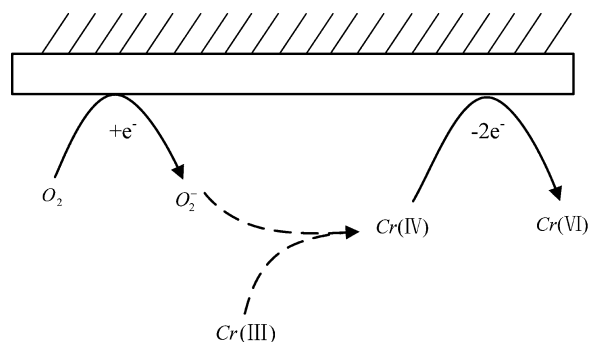
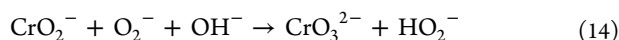


Figure 7. The schematic representation of indirect oxidation of Cr(III) by in situ generated superoxide in KOH solutions.

proposed mechanism of indirect Cr(III) oxidation by in situ generated O_2^- in KOH solutions.



Clearly, the reactivity of O_2^- is enhanced by the alkaline concentration and the HO_2^- fast disproportionation to OH^- , as mentioned in section 3.2.

4. CONCLUSIONS

In this paper, the indirect electro-oxidation of Cr(III) by in situ generation of an chemical oxidation mediator, presumably superoxide, by ORR at a gold electrode has been investigated in KOH solutions using cyclic voltammetry and UV-vis spectroscopy. It is observed that the indirect Cr(III) oxidation behavior is substantially affected by the media alkalinity and there is a pH-modulated ORR process to generate reactive oxygen species as the mediator for Cr(III) oxidation.

The oxygen reduction reaction in KOH solutions is attributed to a quasi-reversible diffusion-controlled reaction. In 0.2 M KOH solution, it is initiated by a 2e reduction to yield HO_2^- , which is fast removed by disproportionation or further reduction to OH^- , leading to a 4e reduction mechanism. Consequently, there is no reactive oxygen species generated for the indirect Cr(III) oxidation. Moreover, the Cr(III) oxidation is frustrated by ORR due to the competition on the electrode active sites. In 3.0 M KOH, the protonation of superoxide is greatly suppressed owing to the increase of OH^- and the decrease of H_2O , and thus, 1e ORR to produce superoxide is dominating. This change in mechanism favors the indirect Cr(III) oxidation through a chemical mediator, superoxide, to oxidize Cr(III) to Cr(IV), which is the rate-determining step of Cr(III) oxidation to Cr(VI).

In summary, it is concluded that the indirect Cr(III) electrochemical oxidation is substantially influenced by KOH concentration. This pH effect, which affects the Cr(III) oxidation mechanism and kinetics, stems from the in situ reactive oxygen species formation via ORR.

AUTHOR INFORMATION

Corresponding Author

*Phone: +86-10-62520910. Fax: +86-10-62520910. E-mail: duhao121@hotmail.com.

Notes

The authors declare no competing financial interest.

ACKNOWLEDGMENTS

Financial support from the National High Technology Research and Development Program of China (863 program) under Grant Nos. 2011AA060704 and 2012BAF03B01, National Natural Science Foundation of China under Grant No. 51090382, and Research Equipments Development Program of Chinese Academy of Sciences is gratefully acknowledged.

REFERENCES

- (1) Fendorf, S. E. *Geoderma* **1995**, *67*, 55–71.
- (2) Dirilgen, N.; Dogan, F. *Ecotoxicol. Environ. Safe* **2002**, *53*, 397–403.
- (3) Eary, L. E.; Rai, D. *Environ. Sci. Technol.* **1987**, *21*, 1187–1193.
- (4) Eary, L. E.; Rai, D. *Environ. Sci. Technol.* **1988**, *22*, 972–977.
- (5) Elderfield, H. *Earth Planet. Sci. Lett.* **1970**, *9*, 10–16.
- (6) Rai, D.; Sass, B. M.; Moore, D. A. *Inorg. Chem.* **1987**, *26*, 345–349.
- (7) Cespon-Romero, M.; Yeburu-Biurru, M. C.; Bermejo-Barrera, M. P. *Anal. Chim. Acta* **1996**, *327*, 37–45.
- (8) Johnson, C. A.; Xyla, A. G. *Geochim. Cosmochim. Acta* **1991**, *55*, 2861–2866.
- (9) Manceau, A.; Charlet, L. *J. Colloid Interface Sci.* **1992**, *148*, 425–442.
- (10) Rodenas, L. A. G.; Iglesia, A. M.; Weisz, A. D.; Morando, P. J.; Belsa, M. A. *Inorg. Chem.* **1997**, *36*, 6423–6430.
- (11) Jin, W.; Moats, M. S.; Zheng, S.; Du, H.; Zhang, Y.; Miller, J. D. *Electrochim. Acta* **2011**, *56*, 8311–8318.
- (12) Tong, J. Y.; King, E. L. *J. Am. Chem. Soc.* **1960**, *82*, 3805–3809.
- (13) Silvester, E.; Charlet, L.; Manceau, A. *J. Phys. Chem.* **1995**, *99*, 16662–16669.
- (14) Landrot, G.; Ginder-Vogel, M.; Sparks, D. L. *Environ. Sci. Technol.* **2010**, *44*, 143–149.
- (15) Rao, L.; Zhang, Z.; Friese, J. I.; Ritherdon, B.; Clark, S. B.; Hess, N. J.; Rai, D. *J. Chem. Soc., Dalton Trans.* **2002**, 267–274.
- (16) Pettine, M.; Gennari, F.; Campanella, L.; Millero, F. *J. Geochim. Cosmochim. Acta* **2008**, *72*, 5692–5707.
- (17) Zhao, Z.; Rush, J. D.; Holcman, J.; Bielski, B. H. *J. Radiat. Phys. Chem.* **1995**, *45*, 257–263.
- (18) Zhang, H.; Bartlett, R. J. *Environ. Sci. Technol.* **1999**, *33*, 588–594.
- (19) Seigneur, C.; Constantinou, E. *Environ. Sci. Technol.* **1995**, *29*, 222–231.
- (20) Panizza, M.; Cerisola, G. *Chem. Rev.* **2009**, *109*, 6541–6569.
- (21) Rodgers, J. D.; Jedral, W.; Bunce, N. J. *Environ. Sci. Technol.* **1999**, *33*, 1453–1457.
- (22) Martinez-Huitle, C. A.; Ferro, S. *Chem. Soc. Rev.* **2006**, *35*, 1324–1340.
- (23) Rajeshwar, K.; Ibanez, J. G.; Swain, G. M. *J. Appl. Electrochem.* **1994**, *24*, 1077–1091.
- (24) Nouri-Nigeh, E.; Permentier, H. D.; Bischoff, R.; Bruins, A. P. *Anal. Chem.* **2010**, *82*, 7625–7633.
- (25) Arellano, C. A. P.; Martinez, S. S. *Int. J. Hydrogen Energy* **2007**, *32*, 3163–3169.
- (26) Jin, W.; Du, H.; Zheng, S.; Xu, H.; Zhang, Y. *J. Phys. Chem. B* **2010**, *114*, 6542–6548.
- (27) Shao, M. H.; Adzic, R. R. *J. Phys. Chem. B* **2005**, *109*, 16563–16566.
- (28) Yeager, E. *Electrochim. Acta* **1984**, *29*, 1527–1537.
- (29) Fei, H.; Leng, W.; Li, X.; Cheng, X.; Xu, Y.; Zhang, J.; Cao, C. *Environ. Sci. Technol.* **2011**, *45*, 4532–4539.
- (30) Johnson, E. L.; Pool, K. H.; Hamm, R. E. *Anal. Chem.* **1966**, *38*, 183–185.
- (31) Zhang, C. Z.; Fan, F.; Bard, A. J. *J. Am. Chem. Soc.* **2009**, *131*, 177–181.
- (32) Zanello, P.; Raspi, G. *Anal. Chim. Acta* **1977**, *88*, 237–243.
- (33) Welch, P.; Hyde, M. E.; Nekrassova, O.; Compton, R. *Phys. Chem. Chem. Phys.* **2004**, *6*, 3153–3159.

- (34) Danlov, F. I.; Velichenko, A. B. *Electrochim. Acta* **1993**, *38*, 437–440.
- (35) Adzic, R. R.; Markovic, N. M.; Vesovic, V. B. *J. Electroanal. Chem.* **1984**, *165*, 105–120.
- (36) Rotzinger, F. P.; Stunzi, H.; Marty, W. *Inorg. Chem.* **1986**, *25*, 489–495.
- (37) Rai, D.; Moore, D. A.; Hess, N. J.; Rosso, K. M.; Rao, L.; Heald, S. M. *J. Solution Chem.* **2007**, *36*, 1261–1285.
- (38) Strbac, S.; Adzic, R. R. *J. Electroanal. Chem.* **1996**, *403*, 169–181.
- (39) Lindenbergh, G.; Simonsson, D. *Electrochim. Acta* **1991**, *36*, 1985–1994.
- (40) Miah, M. R.; Ohsaka, T. *Electrochim. Acta* **2007**, *52*, 6378–6385.
- (41) Kim, J.; Gewirth, A. A. *J. Phys. Chem. B* **2006**, *110*, 2565–2571.
- (42) Davis, R. R.; Horvath, G. L.; Tobias, C. W. *Electrochim. Acta* **1967**, *12*, 287–297.
- (43) Polcyn, D.; Shain, I. *Anal. Chem.* **1966**, *38*, 370–375.
- (44) Hansard, S. P.; Easter, H. D.; Voelker, B. M. *Environ. Sci. Technol.* **2011**, *45*, 2811–2817.